

Differential equations models to study quorum sensing

Judith Pérez-Velázquez^{1,2*} and Burkhard A. Hense^{2†}

¹ *Mathematical Modeling of Biological Systems, Centre for Mathematical Science, Technical University of Munich, Garching, Germany;* ² *Institute of Computational Biology, Helmholtz Zentrum München, Neuherberg, Germany.*

* **Corresponding Author:** Judith Pérez-Velázquez; email: perez-velazquez@helmholtz-muenchen.de

† Deceased February, 28th 2017.

Running Head: Differential equations to study quorum sensing

Key Words: quorum sensing; differential equations; derivatives; ordinary differential equations; partial differential equations; mathematical models.

Abstract

Mathematical models to study quorum sensing (QS) have become an important tool to explore all aspects of this type of bacterial communication. A wide spectrum of mathematical tools and methods such as dynamical systems, stochastics and spatial models can be employed. In this chapter, we focus on giving an overview of models consisting of differential equations (DE), which can be used to describe changing quantities, for example the dynamics of one or more signaling molecule in time and space, often in conjunction with

bacterial growth dynamics. The chapter is divided into two sections: ordinary differential equations (ODE) and partial differential equations (PDE) models of QS. Rates of change are represented mathematically by derivatives, *i.e.* in terms of DE. ODE models allow describing changes in one independent variable, for example time. PDE models can be used to follow changes in more than one independent variable, for example time and space. Both types of models often consist of systems (*i.e.* more than one equation) of equations, such as equations for bacterial growth and autoinducer concentration dynamics. Almost from the onset, mathematical modelling of QS using differential equations has been an interdisciplinary endeavor and many of the works we revised here will be placed into their biological context.

1. Introduction

In this section, we will introduce some basic terminology and concepts concerning mathematical modelling and differential equations. We will try, as much as possible, to place these concepts directly into the context of QS applications.

1.1 Mathematical models

A mathematical model is a representation of a system using mathematical language. A model can be used to describe interactions between components of the system, for example biological interactions. Mathematical models are often simplified representations of a real system, which allow us to understand its essential features. Models can be used to test a hypothesis of how a system works, to try to estimate how a certain event could affect the system (for example the introduction of a therapy) or in general to deduce the consequences of the interactions depicted by the model. Studying and analyzing such models is usually more time and resource effective than constructing real-life systems for the same purpose.

Typically, a model is composed of independent variables, *e.g.* time t , and dependent (on the independent variable(s)) variables, for example autoinducer concentration depending on time $A(t)$. An independent variable causes a change in a dependent variable. A dependent variable can depend on one or more independent variables, for example time and space. Models often also contain parameters, which are fixed values (*e.g.* gravitational constant) or can be varied under experimental conditions (*e.g.* growth rate of the bacteria strain under consideration or diffusion rate of a molecule). Different parameter values can lead to qualitative changes in the system behavior.

The mathematical modelling process often starts with a real-life problem and consists of transforming it to a mathematical problem, which can be solved using mathematical methods. The solution should then be interpreted in terms of the original problem so that it can provide answers and allow to make predictions (Fig. 1).

Note that for reasons of simplicity we will refer to all types of QS signal molecules with the generic name autoinducers (AIs). Some of the mathematical models presented have been developed for a specific type such as homoserine lactones, but we will not make a difference in these cases.

1.2 Differential equations

Differential equations (DE) are mathematical tools to study changes. While an equation in general involves an unknown, usually a number, a DE contains an unknown which is a function. We use DE as many important principles in science are rules for the way variables change, *i.e.* we usually have some information, given by the laws of science, about the way things change. In the real world, one usually does not have a formula. The formula, in fact, is what one would like to have: the formula is the unknown.

If the unknown function in a DE depends on one independent variable, say time $x(t)$, the

differential equation is called ordinary (ODE), otherwise is called partial (PDE). More formally, a differential equation involves an expression in terms of the function and some of its derivatives. Differential equations are continuous mathematical models; *i.e.* the independent variables are continuous.

Note that whereas the differential equation describes the rate of change of a variable, the solution of a differential equation describes the amount or size of a variable as a function of its independent variable (*e.g.* time). Example: If Equation 1 in Table 1 is for the rate at which the numbers of individuals in a population changes; its solution $y(t)$ is the number of individuals in a population at time t .

In the following, we will discuss some existing mathematical model of QS, which use DE.

We have organized this chapter into two sections: ODE and PDE models of QS. Our aim is to give an overview of the modelling process of QS using DE, so we only present selected models, however, we have elaborated a table (ordered chronologically, by publication year) to give the reader a broad overview of existing mathematical models of QS, when possible placing them in our classification (Table 2).

As many of the models described here use the Michaelis-Menten model, which accounts for the kinetic properties of many enzymes, we give a brief explanation of this principle in Box 1.

2. Ordinary differential equations (ODE) models

The first ODEs models of QS were the almost parallel works of four groups: James and co-workers (1) who developed a model for the QS system of *Vibrio fischeri*, Nilsson and co-workers (2) who did not concentrate in a particular QS system, Dockery and Keener (3) who examined the QS of *Pseudomonas aeruginosa*, and Ward and colleagues (4) who also focused in *V. fischeri*. In this section, we will present a deeper review of three ODE models

of QS which portrait many important features that have become customary to model QS, with many existing models based on the ideas contained in these models. They basically represent two ways to mathematically model QS: (1) the population is divided into QS active and QS inactive population, respectively, and each is represented by an equation; (2) explicit equations to describe bacterial dynamics plus AIs dynamics. To exemplify the first category, we revised the model for *V. fischeri* QS system (4). To the second category belong two models from our group developed to describe the QS of *V. fischeri* (5) and *P. putida* (6), respectively, which we will also discuss in this section. Models described in (1), (2) and (3) all belong to the second category, which in fact became the most common approach to model QS. For a review, see (7). Ward and colleagues (4) developed a model of the QS system of *V. fischeri*, see Fig. 2, which consists of the schematic diagram they considered (Fig. 2a) and the mathematical model they created (Fig. 2b). Their model examines bacterial population growth and AIs (which they denoted by QSMs) dynamics, in view of down-regulated (N_d) and up-regulated (N_u) cells, corresponding to cells with an empty *lux*-box or a complex-bound (formed by AIs and protein, which in diagram they term QSM and QSP, respectively), respectively. The binding of QSM-QSP complex to the *lux*-box induces QS activation from a down-regulated state (shown in grey in Fig. 2a) to an up-regulated state (shown in white in Fig. 2b). The switch is assumed to be regulated with increasing AIs (external) concentration A . In the up-regulated (induced) state, genes involved in bioluminescence, but also in production of AIs are expressed on higher level.

To write a mathematical model from the interactions depicted in the diagram developed in (4), three dynamic (*i.e.* whose value changes with time) quantities were defined: down-regulated (N_d), up-regulated (N_u) cells and AIs concentration (A). We describe here how to obtain the first equation (2a) which appears in Fig. 2b: the down-regulated population divides with a cell-division rate r , the specific growth law they follow is given by function F (which

may depend on the data available). Cell division of up-regulated cells produces on average γ up-regulated and $2-\gamma$ down-regulated cells, assuming that only a proportion of replicated chromosomes contain occupied *lux*-boxes. The portion of the population which goes onto becoming active is then accounted for by the second term (after the minus), it is assumed that up-regulation happens at a rate α . Up-regulated population can down-regulate at a rate β . They included a linear function G to describe the complex formation and *lux*-box binding process.

Experiments were specifically designed to estimate the model parameters, see Fig. 3a. The rapid switch observed in experiments from a population of down-regulated cells to an up-regulated state is captured by their model, see the rapid increase in the numerical simulation, Fig. 3b. They however, questioned whether there is in fact a critical concentration of QSM prompting this switch, their model solutions showed that the behavior is observed without imposing a switch explicitly.

The basic model described in (4) was extended several times, for example in (8).

Kuttler and Hense developed an ODE model for the two main QS systems (*lux* and *ain*) of *Vibrio fischeri* (5) (see in Fig. 4a the diagram considered). They followed the modelling approach described by Müller and colleagues (9) - see next section - for the *lux* system. One of their aims was to check the plausibility of the modelled pathway. They did this by comparing the qualitative behavior of the model with some experimental results for the strains ES114 (10) and MJ1 (11), including different mutants of both strains. The main AIs being considered here are 3OC6HSL, but since the model is for two QS systems, the C8HSL-producing enzyme, AinS also forms part of the model. The dynamical behavior of the model fitted qualitatively well to the experimental findings which showed that the behavior of several strains can be described by the same model system, just by modifying parameters

concerning the binding preferences of the AHL-LuxR polymers to the *lux* box, respectively, the activation of *luxI* transcription.

For an illustration, we present three of their equations (the full system contains 19 in total), in Fig. 4b. We explain how to derive equation 3(a): the AIs in the cytoplasm is produced (by the AIs-producing enzyme (*I*)) at a rate α_i , it is also degraded at a rate γ_c and it can be lost (from the cytoplasm) due to diffusion out of the cell, at a rate \widetilde{d}_1 and it can increase due to diffusion into the cell (\widetilde{d}_2). The equation also considers complex disassociations. Note that there is a natural limitation of AinS production, so they used a Michaelis-Menten approach (see equation 3c, for *s* and Box 1). The equations for the intracellular and the extracellular C8HSL are formed similar to those for 3OC6HSL. They found that the system may possess up to 21 different stationary levels, however, the actual number of stationary levels depends on the given external AIs concentrations, in any case many of these stationary states will be unstable and therefore not experimentally observable.

The last model we will present in this section is a model for the one QS system of *Pseudomonas putida* IsoF. The QS signal molecule in this case is an *N*-acyl-homoserine lactone (AHL). The work of Fekete and colleagues (6) is mentioned here as it produced, to our knowledge, first quantitative information regarding the QS processes by fitting experimental data, for example the rate of production of the signaling molecules or the AIs threshold concentration to achieve activation. This type of quantitative information is often used in mathematical models of QS but it is seldom computed from real data. Secondly, because of this quantitative information, the key role of an AHL-regulated enzyme which degrades AHL in *P. putida* IsoF was identified.

See in Fig. 5a the schematic considered, the main variables are in square boxes (AIs, AIS complex, homoserines), hypothetical components are shown in dashed boxes (*E*, putative lactonase; *E*₂, putative homoserine-degrading enzyme) and the switch variable *z* in a dotted

box. The basic mathematical model is presented in Fig. 5b, it consisted of an equation describing AIs (here denoted as A , corresponding in this case to 3-oxo-C10-HSL) net production (involving a Hill-type function, *i.e.* Michaelis-Menten dynamics, see Box 1), which contains a background production of AIs (α), a positive feedback loop leading to an increased production rate of AIs (β), influenced by the actual AIs concentration A , especially if exceeding a certain threshold A_{thresh} , and an abiotic degradation term γ . They further have equations for bacterial population density (N), concentration of AIs-degrading enzyme (E), concentration of first AI-degradation product homoserine HS (S), complexes $[RA]$, concentration of the HS-degrading enzyme (E_2) and enzyme production (z). The model possesses bi-stability (stable resting state and stable active) with the possibility of hysteresis. They investigated how the homoserines and the homoserine-degrading enzymes E and E_2 interact. They further describe the complete AIs-controlling circuit (five equations, Fig. 5b) suggesting that AHL degradation is an integral part of the whole AI circuit of *P. putida* IsoF. See in Fig.6 possible outcomes of AHL time dynamics assuming possible AIs degradation, under a high abiotic degradation rate the AIs dynamics can be affected to the point of almost no AIs present (dotted line). However, this is not what is observed experimentally. Accumulation (dashed line) is neither observed. Therefore, a middle ground of abiotic degradation must be present. If we also assume there is AIs degradation through lactonase (an enzyme actively degrading AIs) we obtained a time course more similar to the one observed experimentally (solid line). *P. putida* QS system has further been studied for continuous cultures (12). Surprisingly, the mathematical analysis showed constant and similar values to those reported for batch cultures, indicating the stability of the system under different environmental conditions.

3. Partial differential equations models of QS

Koeber and co-workers developed a PDE model for the early stages of an infection caused by *Pseudomonas aeruginosa* in burn wounds (13). They modeled only the primary QS system in *P. aeruginosa*. i.e. AIs are 3-oxo-C12-HSL. Their equations involve the concentration of AIs (3-oxo-C12-HSL) in time and space, $A(x, t)$, the density of up-regulated cells $N_u(x, t)$ and down-regulated cells $N_d(x, t)$. They basically used a previously described modeling framework (4) to include space. Population growth is modelled by a logistic expression. They assume that bacteria are in a zone of colonization within the wound (see Fig. 7a). Note how their equation describes changes in space and time through the partial derivative sign ∂ , instead of a d (like in previous section), this sign means that one can describe changes in either of the two variables, time or space; depending which of the variables is next to the sign, in the case of the equations shown, the changes describe changes in time.

The model addresses the effect of space on QS and the infection process. The model described in (13) could be used to compare treatments, for example topical versus blood-delivered agents. They divide the wound into two regions: the bacterial zone, and the uncolonized wound zone (see Fig.7a). QS molecules are produced in the bacterial zone and then diffuse into the surrounding areas. The equations describing the QS molecules concentration in the wound will be different in each region, for illustration purposes we only show the equations related to the bacterial region (see Fig. 7b). Note how model in Fig. 7b is very similar to that of Fig. 3b, that is, the model described in (4) was extended to include time and space. In Fig. 8, the evolution of (a) the AIs concentration and (b) the up-regulated cell fraction of cells in one dimension found between $z = 0.4$ and $z = 0.6$ (bacterial layer location) are shown. The total wound width is $2L$, and the wound depth (uncolonized wound plus bacterial layer) is $l - z_l$. Fig. 8 is meant to show how the model is able to display the rapid rise in A and N_u (at $t = 16$), which corresponds to quorum being reached. They used a PDE (spatial) system as they wanted to investigate whether the presence of a subdermal

plexus in partial thickness burn wounds has a significant effect on the dissemination of AIs in the wound environment. They concluded that, because QS depends upon diffusible signaling molecules, the wound environment plays a critical role in how the initial stages of infection develop.

Müller and colleagues (9) introduced a multi-scale model of QS, *i.e.* a model considering the QS dynamics within the cell and how this reflects at the population level once a cell is QS activated. Their modeling approach starts describing the QS dynamics of a single-cell to later consider a spatially structured model for a cell population. Their model is based on the *V. fischeri* QS system but can be adopted to other systems (as done in (6) for *P. putida*) and contains two parts: within the cell (basically the regulatory pathway, see Fig. 9a) and among cells (the communication). For within the cell, they considered that there is a certain background amount of LuxI and AHL present in the cytoplasm; that AHL diffuses in and out of the cell and that a complex with the receptor molecule LuxR is formed in the cytoplasm. They obtained a basic model for the mass of AIs outside of the cell x_e and mass of AIs within the cytoplasm x_c . See Fig. 9b for the model equations of the single cell model, where the QS term has the familiar form:

$$f(x_c) = \left(\alpha + \frac{\beta x_c^n}{x_{thresh}^n + x_c^n} \right) - \gamma x_c$$

which contains a background production of AHL (α), a positive feedback loop leading to an increased production rate of AHL (β), influenced by the actual AHL concentration, especially if exceeding a certain threshold x_{thresh} , n denotes the degree of polymerization and also there is an abiotic degradation term γ . See equations in Fig. 5b.

They later combined the two parts (single cell and population level) which results in a model with spatial structure, *i.e.* they combine the ODE model (Fig. 9b) with spatial structure by considering the influx/efflux of AIs through the cell membrane. They also include diffusion of AIs in the medium outside the cell.

Note, despite equations in Fig. 9b are ODE, the complete model is a spatial model which includes PDE, which we do not include as its complexity reaches far beyond the scope of this chapter. We mention this model as it offers an innovative approach to include several scales (temporal and spatial) involved in QS.

See in Fig. 10 an example of their results. Circles denote the measured location of producers (they are black if the model predicts activation while grey dots represent resting producer cells). Plus signs mark the measured location of resting, cross signs that of active detector cells. The equipotential lines denote the density of AHL concentration predicted by the model. Their aim was to develop a model to analyze spatial data about individual cells. Even if the model contains a lot of simplifications, their results are able to show the possible loss of the ability of the detector cells to become activated and the importance of boundary effects. Their model can potentially be used to reveal information about communication distances and intercellular variability.

Hense and colleagues studied how AIs regulation may generate spatially heterogeneous behavior (14). The motivation of this model was the fact that in biofilms or colonies, spatial gradients of AIs may emerge which can result in an inhomogeneous AIs induction. They developed a 3D model of AIs regulation in attached microcolonies. They focus on the influence of nutrients on an AIs system. This is a PDE model containing an equation for a generic nutrient $N(x,t)$, the AHL concentration $A(x,t)$ and involving implicitly the cell concentration.

See in Fig. 11 their model, note how their equations also describe changes in space and time through the partial derivative sign ∂ . They based their assumptions on data of the lux AIs system in *Vibrio fischeri*. The cells they considered possess an AIs system of lux-type. $N(x,t)$ is a generic nutrient which is 100 % available. The nutrient follows a Michaelis-Menten dynamics (see equation 7(a) in Fig. 11 and Box 1) and diffuses, generating nutrients

gradients. The symbol ΔA denotes the second derivative of A with respect to space and it is used in modelling to denote diffusion of A . As this symbol appears in both equation 7(a) and (b), it means that both the nutrient and the AIs are assumed to be diffusing. It normally is accompanied by a rate of diffusion (D_A in equation 7(b)) which denotes how fast does A diffuse. Following Hense et al usual modelling approach, they use a constant production rate to indicate AHL basic production, and a Hill function that corresponds to the increased production rate in the induced state (see term involving α and β in equation 7b, similar to (9), and Box 1).

In order to understand the effect of nutrient availability on AHL production, they simulate the system with and without influence of nutrient on the AHL production. They simulated the

mathematical model with $(f(N) = \frac{N_1 N_{N,1}^n}{N_{\tau,1}^{2n} + N^{2n}} + \frac{N_2 N_{N,2}^n}{N_{\tau,2}^{2n} + N^{2n}})$ and without $(f(N)=1)$

influence of nutrient on AIs production (see Fig. 12). They found that, depending on colony size, the maximum activation may be at the colony center, somewhere between colony center and colony boundary, or at the colony boundary. Other models of AI regulation without influence of additional factors such as nutrients usually predict highest activity only in the center.

4. Concluding remarks

Mathematical modelling of QS has proved to be a valuable tool to explore specific aspects of this type of bacterial communication (7). As many of the events involved in activation are dynamic (change with time), DE are an *ad hoc* instrument to help describe interactions between the many players involved. Closely tracking AIs concentration changes has led to a better understanding of the regulation mechanism, in species with many signaling molecules the possibilities are many and DE can help discern distinct contributions. We remark, however, that DE represent one mathematical approach, namely deterministic, where the

outcome is determined through the relationships given to the variables involved, without any room for random variation. In contrast, stochastic models use ranges of values for variables in the form of probability distributions. This approach has also been successfully used to model certain aspects of QS.

Numerical simulations and mathematical analysis have shown that there are a series of common characteristics when it comes to QS. From the modelling viewpoint, Fujimoto and Sawai argued that AI circuits typically found in bacteria generally originate from two distinct forms of bistability (15). Brown, however, discussed that some models fail to satisfy physical constraints and presented canonical models for both Gram-negative and Gram-positive QS systems, which can be applied in well-mixed and biofilm populations (16). Hense and Schuster described properties common to all AI systems (17), allowing for a deeper understanding of their ecological and evolutionary functions. Overall, the original idea of AI systems as a cell density-dependent process giving rise to synchronous behavior is, considering the current state of knowledge about QS, far from adequate. The presented models are instances that mathematical modelling is contributing towards improving our comprehension of this complex regulation system. As theoretical biologists, we are hopeful that this continues to be the case.

References

1. James S, Nilsson P, James G, Kjelleberg S, Fagerström T (2000) Luminescence control in the marine bacterium *Vibrio fischeri*: an analysis of the dynamics of *lux* regulation. *J Mol Biol* 296:1127-1137.
2. Nilsson P, Olofsson A, Fagerlind M, Fagerström T, Rice S, Kjelleberg S, et al (2001) Kinetics of the *ahl* regulatory system in a model biofilm system: how many bacteria constitute a “quorum”? *J Mol Biol* 309:631-640.

3. Dockery J, Keener J (2001) A mathematical model for quorum sensing in *Pseudomonas aeruginosa*. Bull Math Biol 63:95-116.
4. Ward JP, King JR, Koerber AJ, Williams P, Croft JM, Sockett RE (2001) Mathematical modelling of quorum sensing in bacteria. Math Med Biol 18:263-292.
5. Kuttler C, Hense BA (2008) Interplay of two quorum sensing regulation systems of *Vibrio fischeri*. J Theor Biol 251:167-180.
6. Fekete A, Kuttler C, Rothballer M, Hense BA, Fischer D, Buddrus-Schiemann K, et al (2010) Dynamic regulation of *N*-acyl-homoserine lactone production and degradation in *Pseudomonas putida* IsoF. FEMS Microbiol Ecol 72:22-34.
7. Pérez-Velázquez J, Gölgeli M, García-Contreras R (2016) Mathematical modelling of bacterial quorum sensing: a review. Bull Math Biol 78:1585-1639.
8. Ward JP, King JR, Koerber AJ, Croft JM, Sockett RE, Williams P (2004) Cell-signalling repression in bacterial quorum sensing. Math Med Biol 21:169-204.
9. Müller J, Kuttler C, Hense BA, Rothballer M, Hartmann A (2006) Cell-cell communication by quorum sensing and dimension-reduction. J Math Biol 53:672-702.
10. Lupp C, Urbanowski M, Greenberg EP, Ruby EG (2003) The *Vibrio fischeri* quorum-sensing systems *ain* and *lux* sequentially induce luminescence gene expression and are important for persistence in the squid host. Mol Microbiol 50:319-331.
11. Kuo A, Callahan SM, Dunlap PV (1996) Modulation of luminescence operon expression by *N*-octanoyl-L-homoserine lactone in *ainS* mutants of *Vibrio fischeri*. J Bacteriol 178:971-976.
12. Buddrus-Schiemann K, Rieger M, Mühlbauer M, Barbarossa MV, Kuttler C, Hense BA, et al (2014) Analysis of *N*-acylhomoserine lactone dynamics in continuous cultures of *Pseudomonas putida* IsoF by use of ELISA and UHPLC/qTOF-MS-derived measurements and mathematical models. Anal Bioanal Chem 25:6373-6383.

13. Koerber AJ, King JR, Ward JP, Williams P, Croft JM, Sockett RE (2002) A mathematical model of partial-thickness burn-wound infection by *Pseudomonas aeruginosa*: quorum sensing and the build-up to invasion. Bull Math Biol 64:239-259.
14. Hense BA, Müller J, Kuttler C, Hartmann A (2012) Spatial heterogeneity of autoinducer regulation systems. Sensors 12:4156-4171.
15. Fujimoto K, Sawai S (2013) A design principle of group-level decision making in cell populations. PLoS Comput Biol 9:1-13.
16. Brown (2013) Linking molecular and population processes in mathematical models of quorum sensing. Bull Math Biol 75:1813-1839.
17. Hense BA, Schuster M (2015) Core principles of bacterial autoinducer systems. Microbiol Mol Biol Rev 79:153-169.

Figure Legends

Figure 1. The process of mathematical modelling; the starting point is a real-life problem.

Figure 2. (a) Schematic diagram of *V. fischeri* QS system. Reproduced with permission. **(b)** model equations from (4).

Figure 3. (a) Numerical results from (4), fitting model to the experimental data. **(b)** Predicted evolution of the up-regulated cell fraction (up-regulated cells divided by total number of cells N_u/N_T). Reproduced with permission.

Figure 4. (a) Schematic diagram of the two QS systems, *ain* and *lux* (5). The dotted line signifies a bacterium cell, *i.e.* the processes shown inside this line take place intracellularly. Reproduced with permission. **(b)** Equations for the concentration of extracellular AIs (in this case 3OC6HSL) (x_e), within the cytoplasm (x_c) and the C8HSL-producing enzyme, AinS (s). LuxI, AinS: synthases of the AIs 3OCHSL resp C8HSL; LuxO, LitR: parts of the regulation pathway of C8HSL. LuxR: 3OCHSL receptor. Note that LuxR also binds (competitively) to

C8HSL. +: promotion, +++: strong promotion, -: inhibition. LitR activates gene expression as a dimer, LuxR-C8HSL resp. LuxR-3OC6HSL activate gene expression as polymers. Both AIs freely diffuse inside and outside the cells, *i.e.* are assumed to be homogeneously mixed intra- and extracellularly.

Figure 5. (a) Schematic diagram of the QS regulation pathway in *Pseudomonas putida*.

Reproduced with permission. (b) mathematical model considered by (6).

Figure 6. A model-predicted time course of AIs, from (6). Reproduced with permission.

Figure 7. (a) Schematic of the general wound geometry, reproduced with permission. (b)

Bacterial region equations from (13). Region $z = 0$ means subdermal network and $z = H$ means outer surface.

Figure 8. Numerical simulations from (13). The evolution of (a) AIs concentration and (b) the up-regulated cell fraction in one dimension. The sequence of curves is evenly spaced in time starting from zero and increasing to steady state. In (b) up-regulated cells are only found between $z = 0.4$ and $z = 0.6$ and no bacteria are present outside this layer). Reproduced with permission.

Figure 9. (a) Scheme of the regulatory pathway considered in (9). Reproduced with permission. (b) Single cell model.

Figure 10. Simulation results of (9). Reproduced with permission.

Figure 11. Model described in (14); $K_{cat,N}$ and $K_{m,n}$: Michaelis-Menten parameters of nutrient consumption.

Figure 12. Simulations from (14). Profiles of AIs production (green curve), concentration (magenta curve) and nutrient concentration (black curve) in colonies of different sizes (vertical line); left: without nutrient influence, right: with nutrient influence.

Table 1. An ordinary differential equation

Rates of change are represented mathematically by derivatives, *i.e.* in terms of differential equations:

Equation 1

$$\frac{dy}{dt} = f(y, t)$$

the d in dy and dt stands for delta or a change in that variable. Indeed, the amount of change of y , dy divided over a time interval dt in which it occurs represents the rate of change of y . In the context of QS, the rate at which the numbers of cells in a bacterial population or AIs concentration changes with time are examples of phenomena involving rates of change.

Table 2. Brief classification of some existing mathematical models of QS.

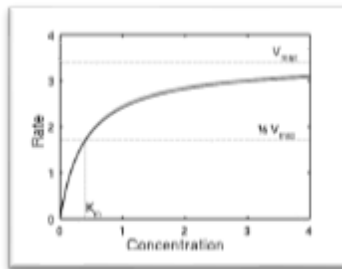
| Year | Author | Bacteria | Method |
|------|--------------------------|--|--------|
| 2000 | James et al | <i>Vibrio fischeri</i> | ODE |
| 2001 | Nilsson et al | Generic | ODE |
| 2001 | Dockery and Keener et al | <i>Pseudomonas aeruginosa</i> | ODE |
| 2001 | Ward et al | <i>V. fischeri</i> | ODE |
| 2002 | Koerber et al | <i>Pseudomonas aeruginosa</i> | PDE |
| 2002 | Ward et al | Generic | PDE |
| 2002 | Chopp et al | <i>Pseudomonas aeruginosa</i> | PDE |
| 2003 | Chopp et al | <i>Pseudomonas aeruginosa</i> | PDE |
| 2003 | Fagerlind et al | <i>Pseudomonas aeruginosa</i> | ODE |
| 2004 | Ward et al | <i>Pseudomonas aeruginosa</i> and <i>Agrobacterium tumefaciens</i> | ODE |
| 2004 | Kuznetsov et al | Generic | ODE |
| 2004 | Viretta et al | <i>Pseudomonas aeruginosa</i> | ODE |
| 2004 | You et al | <i>E. coli</i> | ODE |
| 2004 | Gustafsson et al | <i>Staphylococcus aureus</i> | ODE |
| 2005 | Garcia et al | <i>E. coli</i> | ODE |
| 2004 | Anguige et al | <i>Pseudomonas aeruginosa</i> | ODE |
| 2006 | Goraychev et al | Generic | ODE |
| 2005 | Fagerlind et al | <i>Pseudomonas aeruginosa</i> | ODE |
| 2005 | Anguige et al | <i>Pseudomonas aeruginosa</i> | PDE |
| 2006 | Muller et al | Generic | PDE |
| 2006 | Anguige et al | <i>Pseudomonas aeruginosa</i> | PDE |
| 2007 | Karlsson et al | <i>Streptococcus pneumoniae</i> | ODE |
| 2007 | Hense et al | Generic | ODE |
| 2008 | Williams et al | Generic | ODE |
| 2008 | Kuttler | <i>Vibrio fischeri</i> | ODE |
| 2008 | Müller et al | Generic | ODE |
| 2009 | Janakiraman et al | <i>Pseudomonas aeruginosa</i> | PDE |
| 2010 | Fekete et al | <i>Pseudomonas putida</i> | ODE |
| 2010 | Frederick et al | Generic | PDE |
| 2010 | Jabbari et al | <i>Staphylococcus aureus</i> | ODE |
| 2010 | Vaughan et al | <i>Pseudomonas aeruginosa</i> | PDE |
| 2010 | Barbarossa et al | <i>Pseudomonas putida</i> | ODE |
| 2011 | Frederick et al | Generic | PDE |
| 2012 | Müller et al | Generic | ODE |
| 2012 | Ward et al | Generic | PDE |
| 2012 | Liu et al | <i>Vibrio harveyi</i> | ODE |
| 2012 | Meyer et al | <i>Pseudomonas putida</i> | ODE |
| 2012 | Hense et al | Generic | PDE |
| 2013 | Hunter et al | <i>Vibrio harveyi</i> and <i>Vibrio cholerae</i> | ODE |
| 2013 | Fujimoto and Sawai | Generic | ODE |
| 2013 | Anand et al | <i>Vibrio fischeri</i> | ODE |
| 2013 | Brown | Generic | ODE |
| 2014 | Gölgeli et al | Generic | PDE |
| 2014 | Langebrake et al | <i>Aliivibrio fischeri</i> | PDE |
| 2015 | Emerenini et al | Generic | PDE |
| 2016 | Mund et al | Generic | ODE |
| 2016 | Barbarossa et al | <i>Pseudomonas putida</i> | ODE |
| 2016 | Kumberger et al | Generic | ODE |

Box 1. Michaelis-Menten Model

Biochemical reactions in living cells are often catalyzed by enzymes. These enzymes are proteins that bind and subsequently react specifically with other molecules (substrates). In enzyme kinetics, the phenomenon of saturation plays an important role: even for very high substrate concentrations, one does not consider metabolic rates per se but a maximum rate V_{max} . Let us consider an enzymatic reaction: The enzyme (E) forms a complex with the substrate. This complex can again de-couple or the substrate is converted into a product P and the enzyme can cleave again, we can then write an equation describing the rate of the enzymatic reaction, by relating the reaction rate v to $[S]$, the concentration of the substrate S:

$$v = \frac{d[P]}{dt} = \frac{V_{max}[S]}{K_M + [S]}$$

where, P is the product formed, V_{max} represents the maximum rate achieved by the system, at saturating substrate concentration, K_M is the substrate concentration at which the reaction rate is half of V_{max} .



This means: complex formation of the enzyme and substrate quickly goes into its equilibrium (in this case substrate hardly changes and therefore neither the product). Subsequently, the slow dynamics determines the behaviour: substrate is transformed until there is no left.